Supporting Information

The Effect of Local Non-Thermal Plasma Therapy on the Cancer-Immunity Cycle in a Melanoma Mouse Model

Abraham Lin[1,2], Joey De Backer[3], Delphine Quatannens[2], Bart Cuypers[4], Hanne Verswyvel[1,2], Edgar Cardenas De La Hoz[5], Bart Ribbens[5], Vasiliki Siozopoulou[6], Jonas Van Audenaerde[2], Elly Marcq[2], Filip Lardon[2], Kris Laukens[4], Steve Vanlanduit[5], Evelien Smits[2], Annemie Bogaerts[1]*

1. Optimizing NTP treatment intensity for melanoma treatment

In order to determine the optimal NTP treatment parameters, subcutaneous B16F10 melanoma tumors were treated with NTP for 10 seconds at different intensities (defined by the pulse frequency: 500, 700, and 1000 Hz) for 5 consecutive days (n=4-5) and monitored up to day 17 in a small pilot study (**Figure S1**). Compared to the untreated controls (541.6±256.8 mm^3), 700 Hz treatment had the greatest effect on reducing tumor volumes (230.6±96.4 mm^3) on day 17. At a lower treatment intensity (500 Hz), treatment did not affect tumor volume (419.1±127.7 mm^3) and further increase in pulse frequency to 1000 Hz did not benefit therapy response (272.2±131.4 mm^3). Therefore, NTP treatment intensity of 700 Hz was considered the most optimal treatment and was used in all subsequent experiments.

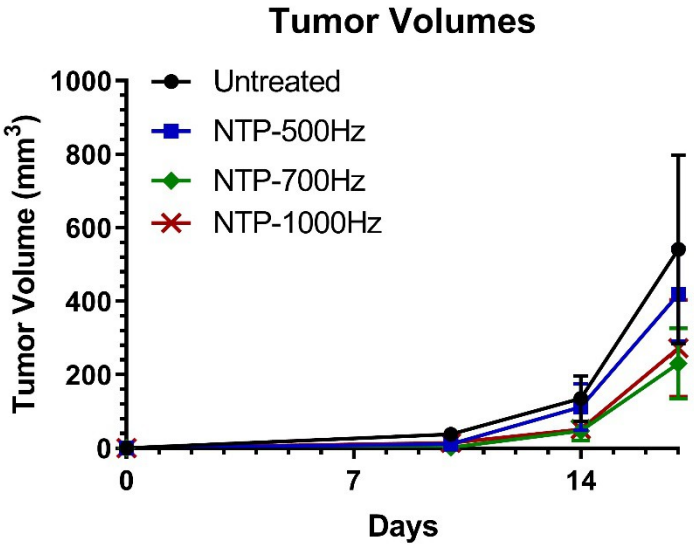

Figure S1. Assessment of the anti-cancer NTP effects at different treatment intensities (defined by the pulse frequency). Subcutaneous melanoma tumors were treated for 5 consecutive days with NTP and monitored up to day 17 (n=4-5).

2. Thermography analysis

2.1 Temperature evolution of NTP treatment for 10 seconds

A video showing the temperature evolution of NTP treatment on the mouse skin, as well as the cooling profile is shown in **Supplementary Video 1**. Images taken immediately after NTP treatment also indicate that no visible damage had occurred during treatment, thus further suggesting that the thermal properties of NTP are not associated with its therapeutic effect (**Figure S2**).

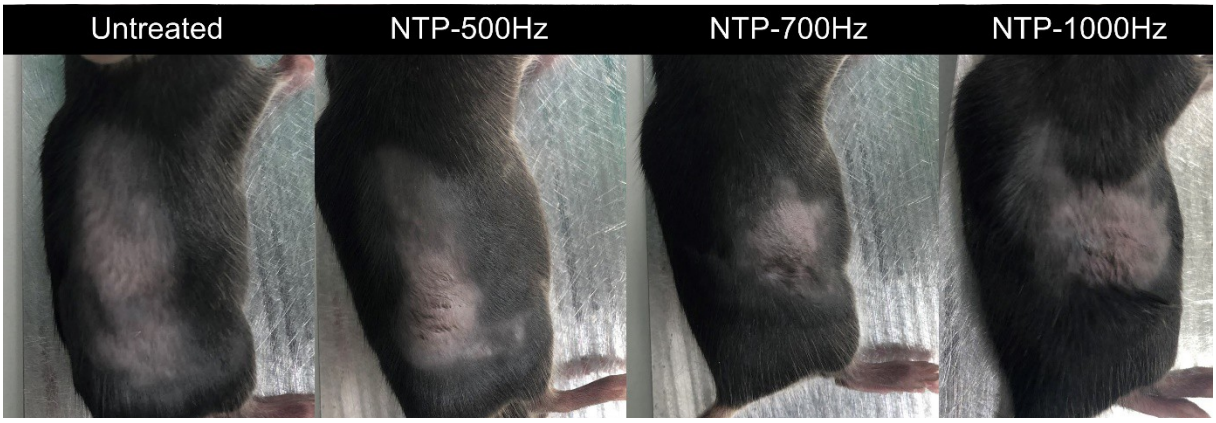

Figure S2. Images of the mouse skin taken after NTP treatment at various treatment intensities (defined by pulse frequency). The hair was removed and NTP was discharged directly onto the skin of the mouse. No visible or thermal damage was observed following treatment compared to untreated.

2.2 Temperature evolution of NTP treatment for 60 seconds

The effect of NTP treatment over longer application times was also investigated. The temperature of the mouse skin did not increase past 38^{o}C with 60 seconds of NTP treatment and rapidly cooled to baseline when treatment was stopped (**Figure S3a**). A spatial profile from the point directly below the NTP applicator (**Figure S3b**) showed that the temperature of the skin 9 mm from the center of treatment was unaffected (**Figure S3c**). A video showing this temperature evolution is shown in **Supplementary Video 2**.

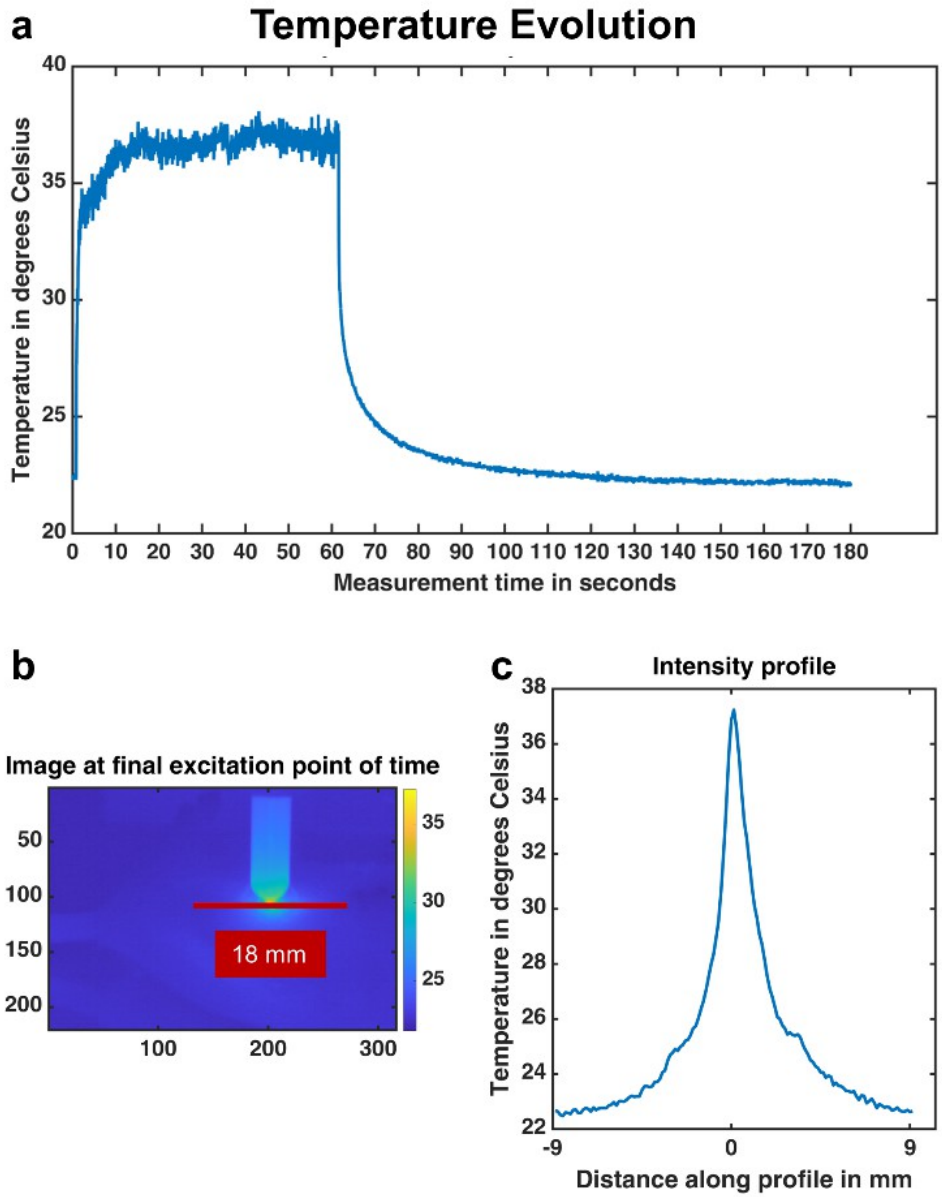

Figure S3. Thermal effects of extended NTP treatment on mouse skin. a) NTP treatment of 60 seconds showed that temperature of the skin below the NTP applicator does not increase past 38°C and cools rapidly when treatment was stopped. b) The temperature of the skin was measured immediately after NTP treatment and c) the spatial profile showed that the temperature of skin 9 mm from the center of treatment was unaffected.

3. RNA sequencing analysis

3.1 GSEA Analysis

A pre-ranked GSEA analysis was performed on RNA sequences from tumors resected on day 7, 10, and 14, comparing that of NTP-treated to untreated controls. A complete list of the upregulated and downregulated hallmark gene sets (adjusted p-value ≤ 0.05) is provided (**Table S1**).

Table S1. Upregulated and downregulated hallmark gene sets

Day 7

NAME	*SIZE*	*NES*	*NOM p-val*	*FDR q-val*	*FWER p-val*	*RANK AT MAX*	*LEADING EDGE*
HALLMARK_CHOLESTEROL_HOMEOSTASIS	64	1.419	0.028	0.518	0.288	3856	tags=55%, list=26%, signal=73%
HALLMARK_E2F_TARGETS	200	1.369	0.004	0.404	0.411	6032	tags=63%, list=40%, signal=103%
HALLMARK_UNFOLDED_PROTEIN_RESPONSE	110	1.300	0.046	0.476	0.616	4495	tags=45%, list=30%, signal=64%
HALLMARK_MYC_TARGETS_V1	200	1.282	0.031	0.418	0.673	6708	tags=69%, list=45%, signal=122%
HALLMARK_INTERFERON_GAMMA_RESPONSE	165	-2.178	0.000	0.000	0.000	2512	tags=70%, list=17%, signal=83%
HALLMARK_INTERFERON_ALPHA_RESPONSE	85	-2.078	0.000	0.000	0.000	1875	tags=73%, list=12%, signal=83%
HALLMARK_MYOGENESIS	143	-2.022	0.000	0.000	0.000	1905	tags=31%, list=13%, signal=36%
HALLMARK_ALLOGRAFT_REJECTION	145	-1.807	0.000	0.000	0.001	1842	tags=49%, list=12%, signal=55%
HALLMARK_IL6_JAK_STAT3_SIGNALING	56	-1.647	0.008	0.003	0.023	3165	tags=54%, list=21%, signal=68%
HALLMARK_IL2_STAT5_SIGNALING	156	-1.614	0.000	0.005	0.043	2981	tags=33%, list=20%, signal=41%
HALLMARK_INFLAMMATORY_RESPONSE	131	-1.499	0.002	0.022	0.190	2144	tags=36%, list=14%, signal=41%
HALLMARK_COMPLEMENT	144	-1.429	0.016	0.049	0.424	3211	tags=42%, list=21%, signal=52%

Day 10

NAME	*SIZE*	*NES*	*NOM p-val*	*FDR q-val*	*FWER p-val*	*RANK AT MAX*	*LEADING EDGE*
HALLMARK_OXIDATIVE_PHOSPHORYLATION	137	2.034	0.000	0.000	0.000	939	tags=52%, list=18%, signal=62%
HALLMARK_HYPOXIA	103	2.012	0.000	0.000	0.000	393	tags=35%, list=8%, signal=37%
HALLMARK_MTORC1_SIGNALING	154	2.011	0.000	0.000	0.000	634	tags=26%, list=12%, signal=29%
HALLMARK_FATTY_ACID_METABOLISM	76	1.934	0.000	0.000	0.000	743	tags=34%, list=14%, signal=39%
HALLMARK_GLYCOLYSIS	107	1.910	0.000	0.000	0.000	592	tags=31%, list=11%, signal=34%
HALLMARK_MYC_TARGETS_V1	177	1.777	0.000	0.001	0.006	1252	tags=46%, list=24%, signal=58%
HALLMARK_HEME_METABOLISM	85	1.711	0.003	0.004	0.025	533	tags=26%, list=10%, signal=28%
HALLMARK_INTERFERON_ALPHA_RESPONSE	38	1.703	0.003	0.004	0.028	682	tags=39%, list=13%, signal=45%
HALLMARK_XENOBIOTIC_METABOLISM	65	1.671	0.002	0.005	0.045	857	tags=28%, list=16%, signal=33%
HALLMARK_P53_PATHWAY	84	1.656	0.000	0.006	0.055	971	tags=32%, list=19%, signal=39%
HALLMARK_INTERFERON_GAMMA_RESPONSE	77	1.625	0.000	0.008	0.086	682	tags=29%, list=13%, signal=32%
HALLMARK_PI3K_AKT_MTOR_SIGNALING	64	1.599	0.008	0.010	0.111	355	tags=17%, list=7%, signal=18%
HALLMARK_UNFOLDED_PROTEIN_RESPONSE	84	1.479	0.010	0.040	0.399	850	tags=23%, list=16%, signal=27%
HALLMARK_ADIPOGENESIS	115	1.477	0.016	0.037	0.401	697	tags=23%, list=13%, signal=26%
HALLMARK_UV_RESPONSE_UP	83	1.356	0.045	0.099	0.795	666	tags=20%, list=13%, signal=23%
HALLMARK_EPITHELIAL_MESENCHYMAL_TRANSITION	89	-2.139	0.000	0.000	0.000	427	tags=39%, list=8%, signal=42%
HALLMARK_COAGULATION	43	-1.754	0.003	0.007	0.016	381	tags=26%, list=7%, signal=27%
HALLMARK_MYOGENESIS	65	-1.716	0.000	0.011	0.033	551	tags=26%, list=11%, signal=29%
HALLMARK_UV_RESPONSE_DN	78	-1.669	0.005	0.014	0.059	575	tags=27%, list=11%, signal=30%
HALLMARK_MITOTIC_SPINDLE	143	-1.355	0.027	0.226	0.699	711	tags=23%, list=14%, signal=26%

Day 14

NAME	*SIZE*	*NES*	*NOM p-val*	*FDR q-val*	*FWER p-val*	*RANK AT MAX*	*LEADING EDGE*
HALLMARK_MYC_TARGETS_V1	200	1.874	0.000	0.002	0.002	1307	tags=40%, list=11%, signal=44%
HALLMARK_E2F_TARGETS	199	1.750	0.000	0.031	0.034	1332	tags=35%, list=11%, signal=38%
HALLMARK_MYC_TARGETS_V2	57	1.589	0.046	0.119	0.182	2147	tags=63%, list=18%, signal=77%

HALLMARK_FATTY_ACID_METABOLISM	128	1.508	0.006	0.155	0.284	409	tags=5%, list=4%, signal=5%
HALLMARK_PEROXISOME	79	1.464	0.074	0.169	0.358	913	tags=14%, list=8%, signal=15%
HALLMARK_G2M_CHECKPOINT	195	1.416	0.017	0.186	0.456	1362	tags=30%, list=12%, signal=34%
HALLMARK_MTORC1_SIGNALING	198	1.344	0.023	0.175	0.591	1261	tags=24%, list=11%, signal=27%
HALLMARK_INTERFERON_GAMMA_RESPONSE	175	-1.785	0.000	0.000	0.000	557	tags=53%, list=5%, signal=54%
HALLMARK_INTERFERON_ALPHA_RESPONSE	90	-1.762	0.000	0.000	0.000	463	tags=69%, list=4%, signal=71%
HALLMARK_IL6_JAK_STAT3_SIGNALING	68	-1.627	0.000	0.003	0.010	542	tags=22%, list=5%, signal=23%
HALLMARK_INFLAMMATORY_RESPONSE	144	-1.621	0.000	0.003	0.013	834	tags=28%, list=7%, signal=30%
HALLMARK_COMPLEMENT	144	-1.607	0.001	0.003	0.020	993	tags=24%, list=9%, signal=26%
HALLMARK_ALLOGRAFT_REJECTION	148	-1.552	0.001	0.010	0.070	807	tags=30%, list=7%, signal=32%
HALLMARK_APOPTOSIS	138	-1.529	0.001	0.015	0.116	1319	tags=25%, list=11%, signal=27%
HALLMARK_COAGULATION	90	-1.502	0.009	0.024	0.203	727	tags=13%, list=6%, signal=14%
HALLMARK_UV_RESPONSE_DN	132	-1.453	0.007	0.049	0.407	610	tags=7%, list=5%, signal=7%
HALLMARK_TNFA_SIGNALING_VIA_NFKB	174	-1.428	0.008	0.062	0.519	1225	tags=22%, list=11%, signal=25%
HALLMARK_IL2_STAT5_SIGNALING	163	-1.386	0.015	0.095	0.720	1089	tags=26%, list=9%, signal=28%
HALLMARK_EPITHELIAL_MESENCHYMAL_TRANSITION	168	-1.364	0.019	0.114	0.819	833	tags=8%, list=7%, signal=9%

NES: normalized enrichment score; NOM p-val: adjusted p-value; FDR q-val: false discovery rate; FWER p-val: family-wise error rate

3.2 Differential Gene Expression (DESeq2) Analysis

Based on the GSEA analysis, we further investigated the genes in the IL6-JAK-STAT3, unfolded protein response, and interferon gamma pathways that were significantly ($p \leq 0.05$) up- or downregulated on day 7, 10, and 14 (**Table S2**). Due to the high variability within the mice, the adjusted p-values did not reveal any significant genes, and therefore, the uncorrected p-values and log2fold change values (Log2FC) are provided. These results should, therefore, be interpreted with care, and increasing the number of mice per group would help provide more concrete insight.

Table S2. Genes in the selected pathways that were upregulated or downregulated

IL6-JAK-STAT3

DAY 7			**Day 10**			**Day 14**		
Gene	*Log2FC*	*p-value*	*Gene*	*Log2FC*	*p-value*	*Gene*	*Log2FC*	*p-value*
IL12RB1	-1.832	0.0705	IL6ST	-0.2571	0.0045	Itgb3	-0.6963	4.85E-08
STAT1	-0.882	0.1805	CBL	-0.2151	0.0197	Tyk2	-0.2327	0.0017
TNF	-0.830	0.1916	ITGA4	-0.2697	0.0354	Il12rb1	-2.5049	0.0021
STAT2	-0.944	0.1932	OSMR	-0.6945	0.1022	Tnf	-1.1278	0.0210
IRF1	-0.925	0.2319	CSF2RA	-0.5589	0.1128	Stat2	-1.1150	0.0233
CXCL9	-0.955	0.2418	IL1R1	-1.1327	0.1174	Jun	-0.3905	0.0371
IL2RG	-1.028	0.2997	PF4	-0.8373	0.1627	Cxcl9	-2.4841	0.0395
SOCS1	-0.659	0.4365	CD14	-0.9670	0.1649	Stat1	-1.2806	0.0423

CXCL10	-0.684	0.4385	TLR2	-0.6513	0.1667	IRF1	-1.7070	0.0447
IL2RA	-0.605	0.4892	IL12RB1	0.6042	0.1752	CNTFR	0.2303	0.0457
			CCL7	-0.6657	0.2857	IRF9	-0.7631	0.0603
			PIK3R5	-0.5287	0.3935	IL15RA	-0.8677	0.0818
			CSF2RB	-0.5583	0.3985	SOCS1	-1.3700	0.0954
						MAP3K8	-0.5375	0.1362
						IL2RA	-1.4244	0.1562
						CXCL10	-0.8965	0.2094
						IL2RG	-0.5721	0.3507
						CSF2RB	-0.5208	0.3878
						CSF3R	-0.5685	0.4141

UNFOLDED PROTEIN RESPONSE

DAY 7			**Day 10**			**Day 14**		
Gene	*Log2FC*	*p-value*	*Gene*	*Log2FC*	*p-value*	*Gene*	*Log2FC*	*p-value*
VEGFA	0.6583	0.0191	GOSR2	0.2464	0.0008	SPCS3	0.2125	0.0076
ERO1A	0.5655	0.0481	EIF4EBP1	0.2498	0.0039	SSR1	0.2370	0.0099
			ERO1A	0.4929	0.0047	CALR	0.2265	0.0321
			DDIT4	0.4062	0.0054	EXOSC2	0.1815	0.0453
			EIF4A3	0.1968	0.0180			
			HSPA9	0.2128	0.0297			
			H2AX	0.2244	0.0329			
			CXXC1	-0.1469	0.0407			
			EIF4A1	0.1121	0.0433			
			NOP56	-0.1647	0.0488			
			ATP6V0D1	0.1725	0.0488			
			SEC11A	0.2217	0.0491			

INTERFERON GAMMA

Day 7			**Day 10**			**Day 14**		
Gene	*Log2FC*	*p-value*	*Gene*	*Log2FC*	*p-value*	*Gene*	*Log2FC*	*p-value*
NLRC5	-1.1418	0.0622	IFI27	0.4000	0.0059	HELZ2	-0.8278	0.0006
RNF213	-0.8380	0.1077	PFKP	0.3182	0.0070	ZNFX1	-0.4797	0.0036
TAP1	-1.1387	0.1389	UBE2L6	0.8084	0.0087	ADAR	-0.5821	0.0048
BST2	-0.8724	0.1424	NAMPT	0.3264	0.0108	SAMD9L	-0.8436	0.0086
GBP6	-1.4343	0.1435	BST2	0.4497	0.0133	IFI27	-0.5449	0.0115
B2M	-0.8436	0.1516	NCOA3	-0.2523	0.0211	DDX58	-1.0325	0.0133
TAPBP	-0.9466	0.1731	PSMB2	0.2188	0.0383	PML	-0.3744	0.0169
PSME1	-0.6909	0.1782	PLSCR1	0.2033	0.0440	STAT2	-1.1150	0.0233
LGALS3BP	-0.6387	0.1850	PSMA2	0.1782	0.0466	RSAD2	-1.2412	0.0238
STAT2	-0.9442	0.1932	TAP1	0.5926	0.1588	IFITM2	0.2086	0.0245
IFITM3	-0.8949	0.2090	LY6E	-0.5632	0.3677	TRIM25	-0.7181	0.0279
PARP12	-0.7404	0.2141	GBP6	0.5554	0.4007	PARP14	-1.6582	0.0293
PARP14	-0.9491	0.2176	SERPING1	-0.6143	0.4154	GBP6	-2.6723	0.0302
UBE2L6	-0.9185	0.2263				OGFR	-0.3453	0.0327
ZNFX1	-0.5331	0.2269				TAPBP	-1.3173	0.0331

CXCL9	-0.9551	0.2418		PARP12	-1.1176	0.0343
SAMHD1	-0.9275	0.2427		NLRC5	-1.9799	0.0392
CD74	-1.1967	0.2444		CXCL9	-2.4841	0.0395
SAMD9L	-0.6074	0.2455		LAP3	-0.4080	0.0461
LAP3	-0.5951	0.2580		UBE2L6	-1.3170	0.0470
IRF2	-0.5628	0.2593		IFITM3	-0.8906	0.0486
RSAD2	-0.5874	0.4086		IRF2	-0.3023	0.0488
CXCL10	-0.6842	0.4385		RNF213	-0.9596	0.0532
				TAP1	-1.8648	0.0568
				IRF9	-0.7631	0.0603
				B2M	-1.0038	0.0649
				PSME1	-0.8148	0.0740
				LGALS3BP	-0.5764	0.0861
				BST2	-0.9201	0.1174
				CD74	-1.2132	0.1771
				CXCL10	-0.8965	0.2094
				SAMHD1	-0.5023	0.2339
				SERPING1	-0.5226	0.4818

4. Flow cytometry analysis

4.1 DC and NK cell gating strategy

A representative gating strategy to identify dendritic cells (DCs) and natural killer (NK) cells is shown (**Figure S4**).

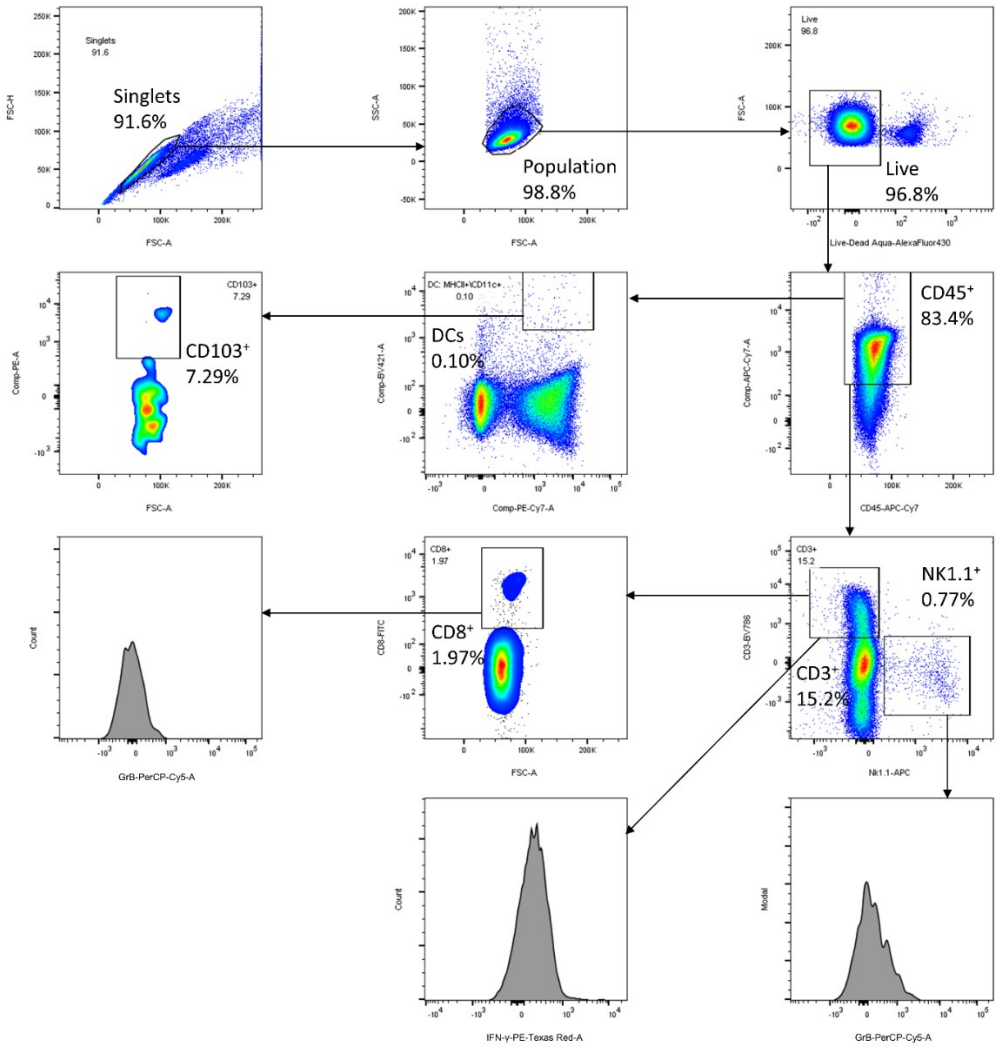

Figure S4. The flow cytometry gating strategy to identify DCs and NK cells along with intracellular interferon-gamma and granzyme b.

4.2 T cell gating strategy

A representative gating strategy to identify $CD8^+$, non-regulatory $CD4^+$, and regulatory T cells is shown (**Figure S5**). The gating strategy to delineate non-exhausted populations of T cells are also shown.

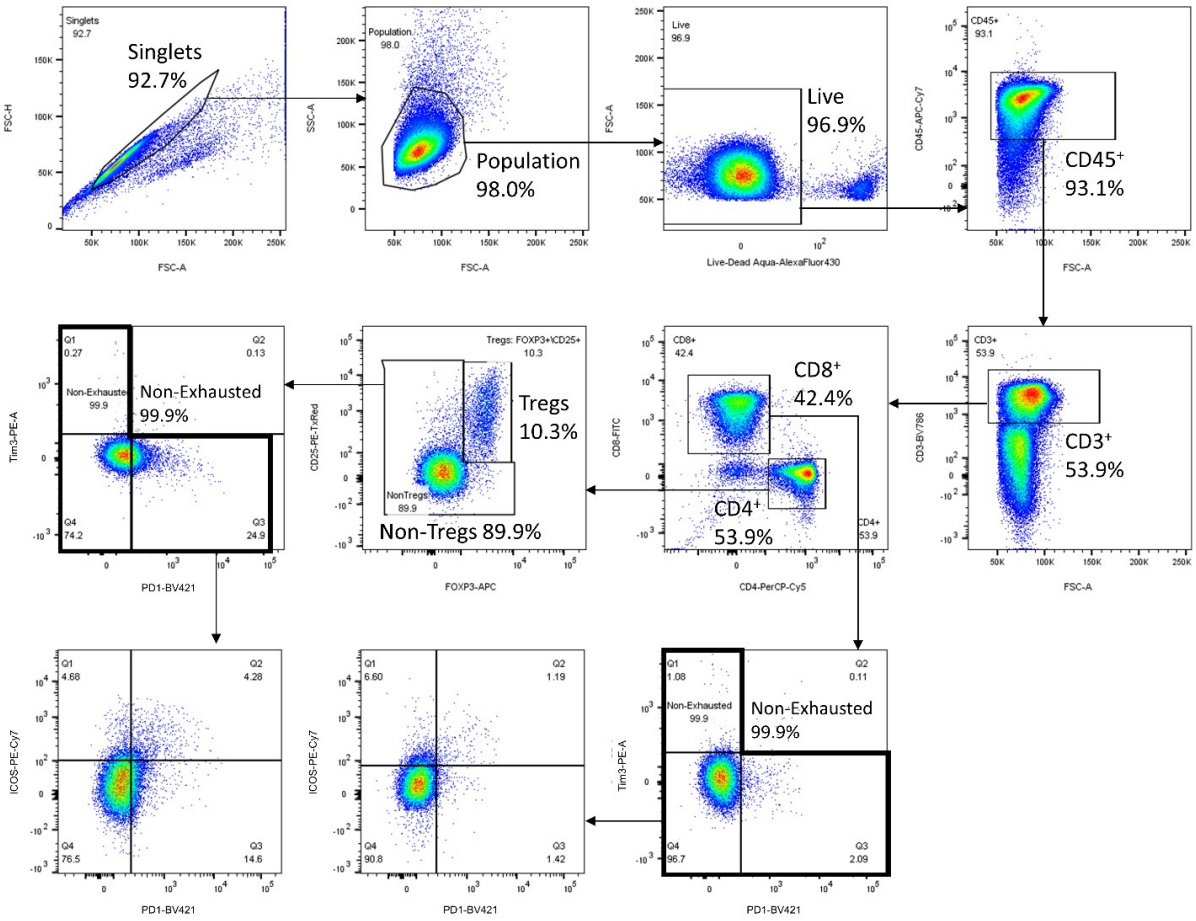

Figure S5. The flow cytometry gating strategy to identify subpopulations of T cells and activation and exhaustion markers.

4.3 NK cell analysis in the tumor and tumor draining lymph node

The population of NK cells in the tumor (**Figure S6a**) and tumor draining lymph node (**Figure S6b**) was evaluated with flow cytometry. NTP treatment did not appear to affect NK cell populations on either day 10 or day 14. Furthermore, overton analysis of IFN-γ with the corresponding isotype also did not show significant differences between the two groups in the tumor or tumor draining lymph node (**Figure S6c**, **d**).

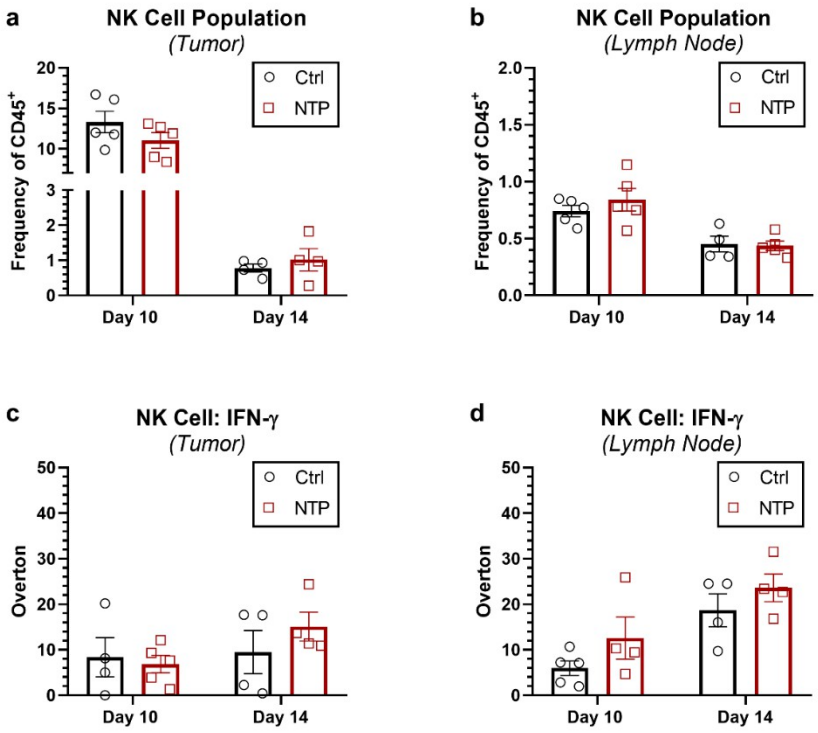

Figure S6. Flow cytometry assessment of NK cells following NTP treatment. The NK cell population in the a) tumor and b) tumor draining lymph node was evaluated on day 10 and 14. Overton analysis of interferon gamma (IFN-γ) expression in the NK cells also did not show significant differences between the NTP-treated and untreated control (Ctrl) groups in the c) tumor or d) lymph node.

5. Detailed Methods

5.1 Flow cytometry panels

The following section describes in detail the antibodies and clones used for flow cytometry analysis (**Table S3**). The T cell panel consisted of CD8-FITC (Clone 53-6.7, Biolegend, The Netherlands), Tim3-PE (Clone 5D12, BD Biosciences, Belgium), CD25-PEDazzle549 (Clone PC61, Biolegend), CD4-PerCP/Cy5.5 (Clone GK1.5, Biolegend), ICOS-PE-Cy7 (Clone C398.4A, Biolegend), FOXP3-APC (Clone FJK-16s, Thermofisher Scientific, United States), CD45.2-APC-Cy7 (Clone 104, BD Biosciences), PD-1-BV421 (Clone RMP1-30, Biolegend), LiveDead Aqua (Life technologies, United States), CD3-BV785 (Clone 17A2, Biolegend). The NK cell and DC panel consisted of CD8-FITC (Clone 53-6.7, Biolegend), CD103-PE (Clone 2E7, Thermofisher Scientific), IFN-γ-PE-Dazzle549 (Clone XMG1.2, Biolegend), GranzymeB-PerCP/Cy5.5 (Clone QA16A02, Biolegend), MHC Class II-

PE/Cy7 (Clone M5/114.15.2, Biolegend), NK1.1-APC (Clone P136, Biolegend), CD45.2-APC-Cy7 (Clone 104, BD Biosciences), CD11c-BV421 (Clone N418, BD Biosciences), CD11c-BV421 (Clone N418, BD Biosciences), CD3-BV785 (Clone 17A2, Biolegend). The samples obtained from the spleens were stained with the following antibody cocktail, CD8-FITC (Clone 53-6.7, Biolegend), CD103-PE (Clone 2E7, Thermofisher Scientific), CD3-PEDazzle594 (Clone 17A2, Biolegend), CD4-PerCP/Cy5.5 (Clone GK1.5, Biolegend), MHC Class II-PE/Cy7 (Clone M5/114.15.2, Biolegend), FOXP3-APC (Clone FJK-16s, Thermofisher Scientific), CD45.2-APC-Cy7 (Clone 104, BD Biosciences), CD11c-BV421 (Clone N418, BD Biosciences), LiveDead Aqua (Life technologies, United States), CD25-BV785 (Clone PC61, Biolegend).

Table S3. Antibodies used for flow cytometry panels

T cell Panel					
Fluor	**Antigen**	**Clone**	**Company**	**Cat No.**	**Dilution**
FITC	CD8	53-6.7	Biolegend	100705	1:50
PE	Tim3	5D12	BDBioscience	566346	1:25
PE-TxRd(dzl549)	CD25	PC61	Biolegend	102048	1:100
PerCP-Cy5	CD4	GK1.5	Biolegend	100434	1:100
PE-Cy7	ICOS	C398.4A	Biolegend	313519	1:25
APC	FOXP3	FJK-16s	Thermofisher	17-5773-82	1:50
APC-Cy7	CD45	104	BD Bioscience	560694	1:50
BV421	PD1	RMP1-30	Biolegend	109121	1:25
AF430	L/D Aqua	-	Thermofisher	L34957	1:50
BV786	CD3	17A2	Biolegend	100231	1:100
DC/NK cell Panel					
Fluor	**Antigen**	**Clone**	**Company**	**Cat No.**	**Dilution**
FITC	CD8	53-6.7	Biolegend	100705	1:50
PE	CD103	2E7	Thermofisher	12-1031-83	1:100
PE-TxRd(dzl549)	IFN-gamma	XMG1.2	Biolegend	505845	1:100
PerCP-Cy5	granzyme B	QA16A02	Biolegend	372212	1:50
PE-Cy7	MHC-II	M5/114.15.2	Biolegend	107630	1:50
APC	NK1.1	PK136	Biolegend	108701	1:50
APC-Cy7	CD45	104	BD Bioscience	560694	1:50
BV421	CD11c	N418	BD Bioscience	565452	1:50
AF430	L/D Aqua	-	Thermofisher	L34957	1:50
BV786/5	CD3	17A2	Biolegend	100231	1:100
Spleen Panel					
Fluor	**Antigen**	**Clone**	**Company**	**Cat No.**	**Dilution**
FITC	CD8	53-6.7	Biolegend	100705	1:50
PE	CD103	2E7	Thermofisher	12-1031-83	1:100
PE-TxRd (dzl549)	CD3	17A2	Biolegend	100246	1:100
PerCP-Cy5	CD4	GK1.5	Biolegend	100434	1:100
PE/Cy7	MHC-II	M5/114.15.2	Biolegend	107630	1:50
APC	FOXP3	FJK-16s	Thermofisher	17-5773-82	1:50
APC-Cy7	CD45.2	104	BD Bioscience	560694	1:50
BV421	CD11c	N418	BD Bioscience	565452	1:50
AF430	L/D Aqua	-	Thermofisher	L34957	1:50
BV786	CD25	PC61	BD Bioscience	564023	1:50

5.2 Optimization of immunofluorescence staining

Tumor slides were stained with the isotype controls of CRT, CD47, and PD-L1 to check for non-specific staining and determine the optimal primary and secondary antibody dilutions. CRT was optimized previously in the lab and here we demontrated a low amount of non-specific binding (**Figure S7a**). Since the stock concentration of the monclonal CRT antibody and the rabbit IgG isotype control was different, the dilutions were made to keep the final staining concentration the same. The starting concentration for the isotypes of CD47 and PD-L1 were to the same, and we found that for CD47, a 1:100 and a 1:200 dilution was most optimal for primary and secondary staining, respectively (**Figure S7b**), while a 1:200 dilution for both primary and secondary staining was most optimal for PD-L1 (**Figure S7c**). These concentrations were used for staining of all tumor slides.

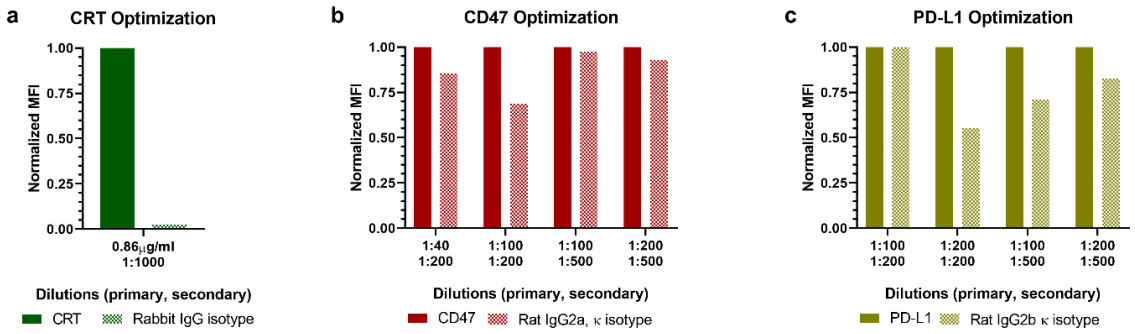

Figure S7. Comparison of primary staining with isotype controls. Data are shown normalized to the primary stain at various dilutions for a) CRT, b) CD47, and c) PD-L1

5.3 Computational image processing

Individual nuclei in the images were indexed using connected component analysis and objects smaller than 40 pixels^2 were removed. The nuclear masks were morphologically dilated using a disk structuring element with diameter of 51 pixels (20.4 μm^2) to form a cytoplasmic mask. Each pixel of the resulting cytoplasmic mask was indexed to the nearest nuclei. In this way, mean signal intensity and positivity for each cell in the approximated cytoplasm was also measured individually. Signal marker positivity for protein expression were imaged fluorescently using red (TxRED) and green (GFP) channels. To

quantify expression of CRT, CD47, and PDL1, the intensity values were corrected for background signal by first saturating the signal to the 95th percentile and subtracting by a one sided low pass filter formed by a Gaussian kernel of 60 pixels in standard deviation. The resultant intensity values for these images were measured using in nuclear and cytoplasmic masks.